



Title	Swallowing-related neural oscillation: an intracranial EEG study
Author(s)	Hashimoto, Hiroaki; Takahashi, Kazutaka; Kameda, Seiji et al.
Citation	Annals of Clinical and Translational Neurology. 2021, 8(6), p. 1224-1238
Version Type	VoR
URL	<a href="https://hdl.handle.net/11094/95626">https://hdl.handle.net/11094/95626</a>
rights	This article is licensed under a Creative Commons Attribution-NonCommercial-NoDerivatives 4.0 International License.
Note	




*The University of Osaka Institutional Knowledge Archive : OUKA*

<https://ir.library.osaka-u.ac.jp/>

The University of Osaka

## RESEARCH ARTICLE

# Swallowing-related neural oscillation: an intracranial EEG study

Hiroaki Hashimoto<sup>1,2,3</sup> , Kazutaka Takahashi<sup>4</sup>, Seiji Kameda<sup>1</sup>, Fumiaki Yoshida<sup>1,5</sup>, Hitoshi Maezawa<sup>1</sup>, Satoru Oshino<sup>6</sup>, Naoki Tani<sup>6</sup>, Hui Ming Khoo<sup>6</sup> , Takufumi Yanagisawa<sup>6</sup> , Toshiki Yoshimine<sup>3</sup>, Haruhiko Kishima<sup>6</sup> & Masayuki Hirata<sup>1,3,6</sup>

<sup>1</sup>Department of Neurological Diagnosis and Restoration, Graduate School of Medicine, Osaka University, Yamadaoka 2-2, Suita, Osaka, 565-0871, Japan

<sup>2</sup>Department of Neurosurgery, Otemae Hospital, Chuo-ku Otemae 1-5-34, Osaka, Osaka, 540-0008, Japan

<sup>3</sup>Endowed Research Department of Clinical Neuroengineering, Global Center for Medical Engineering and Informatics, Osaka University, Yamadaoka 2-2, Suita, Osaka, 565-0871, Japan

<sup>4</sup>Department of Organismal Biology and Anatomy, The University of Chicago, 1027 E 57<sup>th</sup> St, Chicago, IL, 60637

<sup>5</sup>Department of Anatomy and Physiology, Saga Medical School Faculty of Medicine, Saga University, Nabeshima 5-1-1, Saga, Saga, 849-8501, Japan

<sup>6</sup>Department of Neurosurgery, Graduate School of Medicine, Osaka University, Yamadaoka 2-2, Suita, Osaka, 565-0871, Japan

## Correspondence

Hiroaki Hashimoto, Department of Neurological Diagnosis and Restoration, Graduate School of Medicine, Osaka University, Yamadaoka 2-2, Suita, Osaka 565-0871, Japan. Tel: +81-6-6210-8429; Fax: +81-6-6210-8430; E-mail: h-hashimoto@ndr.med.osaka-u.ac.jp  
 Masayuki Hirata, Department of Neurological Diagnosis and Restoration, Graduate School of Medicine, Osaka University, Yamadaoka 2-2, Suita, Osaka 565-0871, Japan. Tel: +81-6-6210-8429; Fax: +81-6-6210-8430; E-mail: mhirata@ndr.med.osaka-u.ac.jp

## Funding Information

This work was supported by the Japan Society for the Promotion of Science (JSPS) KAKENHI [Grant nos. JP26282165 (Masayuki Hirata), JP18H04166 (Masayuki Hirata), JP18K18366 (Hiroaki Hashimoto)], by the Ministry of Internal Affairs and Communications (Masayuki Hirata), by a grant from the National Institute of Information and Communications Technology (NICT) (Masayuki Hirata), and by a grant from the National Institute of Dental and Craniofacial Research (NIDCR)-RO1 DE023816 (Kazutaka Takahashi).

Received: 14 January 2021; Revised: 26 February 2021; Accepted: 2 March 2021

*Annals of Clinical and Translational Neurology* 2021; 8(6): 1224–1238

doi: 10.1002/acn3.51344

## Abstract

**Objective:** Swallowing is a unique movement due to the indispensable orchestration of voluntary and involuntary movements. The transition from voluntary to involuntary swallowing is executed within milliseconds. We hypothesized that the underlying neural mechanism of swallowing would be revealed by high-frequency cortical activities. **Methods:** Eight epileptic participants fitted with intracranial electrodes over the orofacial cortex were asked to swallow a water bolus and cortical oscillatory changes, including the high  $\gamma$  band (75–150 Hz) and  $\beta$  band (13–30 Hz), were investigated at the time of mouth opening, water injection, and swallowing. **Results:** Increases in high  $\gamma$  power associated with mouth opening were observed in the ventrolateral prefrontal cortex (VLPFC) with water injection in the lateral central sulcus and with swallowing in the region along the Sylvian fissure. Mouth opening induced a decrease in  $\beta$  power, which continued until the completion of swallowing. The high  $\gamma$  burst of activity was focal and specific to swallowing; however, the  $\beta$  activities were extensive and not specific to swallowing. In the interim between voluntary and involuntary swallowing, swallowing-related high  $\gamma$  power achieved its peak, and subsequently, the power decreased. **Interpretation:** We demonstrated three distinct activities related to mouth opening, water injection, and swallowing induced at different timings using high  $\gamma$  activities. The peak of high  $\gamma$  power related to swallowing suggests that during voluntary swallowing phases, the cortex is the main driving force for swallowing as opposed to the brain stem.

## Introduction

Swallowing is a primitive and fundamental function, as well as a unique movement because the cooperation between voluntary and involuntary movements is necessary for normal swallowing. Thus, the swallowing movement is divided into two components: voluntary movement and involuntary movement.<sup>1</sup> The cerebral cortex is assumed to play a crucial role in swallowing movements along with the brain stem. The cerebral cortex triggers swallowing and modulates the brain stem, where the central pattern generator (CPG) for swallowing is assumed to be located in humans.<sup>2</sup> Therefore, cerebral cortex damage due to stroke<sup>3</sup> or neurodegenerative disease<sup>4</sup> promotes swallowing disturbance (dysphagia).

The adoption of different postures and modification of the bolus consistency are widely accepted in clinical practice as treatments for dysphagia.<sup>5</sup> Peripheral electrical stimulation, such as pharyngeal electrical stimulation<sup>6</sup> or transcutaneous neuromuscular stimulation,<sup>7</sup> and noninvasive brain stimulation using repetitive transcranial magnetic stimulation (rTMS)<sup>8</sup> or transcranial direct current stimulation (tDCS)<sup>9</sup> are also being studied as emerging therapeutic strategies. Positive effects have been reported for these neuromodulation strategies for dysphagia; however, various intensities and durations have been used for stimulation,<sup>10</sup> and the best conditions for stimulation remain unclear. Therefore, the treatment effects of these neuromodulation therapies remain limited, and further studies are required to provide evidence for overcoming dysphagia.

We have continued to research and contribute to the field of neuromodulation for dysphagia using our brain-machine interface (BMI) technology. First, we developed a novel swallow-tracking system that enabled us to noninvasively monitor swallowing in real time.<sup>11</sup> Next, we demonstrated that deep transfer learning applied to intracranial electroencephalogram (EEG) signals was able to classify swallowing intention well.<sup>12</sup> Current neuromodulation strategies for dysphagia stimulate brain areas or peripheral organs regardless of patients' swallowing intention. We hypothesized that if the stimulation was executed by the patients' swallowing intention, a higher degree of recovery would be obtained by sensory neurofeedback. BMI technology is useful for the realization of stimulation triggered by patients' intention.

The elucidation of swallowing-related neural processing is essential for the realization of such a swallow-assisting BMI. Noninvasive methods, such as scalp EEG,<sup>13</sup> positron emission tomography (PET),<sup>14</sup> near-infrared spectroscopy (NIRS),<sup>15</sup> TMS,<sup>16</sup> functional magnetic resonance imaging (fMRI),<sup>17,18</sup> and magnetoencephalography (MEG),<sup>19,20</sup> implicate multiple cortical sites involved in swallowing.

fMRI has high spatial resolution, in the order of millimeters; however, it has poor temporal resolution.<sup>21</sup> The temporal resolution of MEG is high, in the order of milliseconds<sup>19</sup>; however, its spatial resolution is limited. Noninvasive methods have either weak temporal or spatial resolution; therefore, we inferred that such methods had a potential limitation for the investigation of neural processing related to swallowing that transitions from the voluntary to involuntary phase in the order of milliseconds.<sup>2,22</sup>

Intracranial EEGs (iEEGs), such as electrocorticograms (ECoGs), that record neural activities directly from the cortical surface of the brain enable us to measure neural activities with high spatiotemporal resolution. Moreover, using ECoG, we can measure high-frequency neural oscillations, including high  $\gamma$  bands (>50 Hz). High  $\gamma$  activity is a key oscillation that reflects the neural processing of sensory, motor, and cognitive events.<sup>23–25</sup> High  $\gamma$  activities also show better functional localization than that in lower frequency bands<sup>23</sup> and have come to be known as useful features for decoding neural signals.<sup>12</sup> Here, we hypothesized that the analysis of high  $\gamma$  activities acquired by ECoG measurements would be able to reveal swallowing-related cerebral oscillation changes in the order of milliseconds that have remained unclear. Novel findings may provide neuromodulation strategies for dysphagia with beneficial information, such as brain areas and timing for stimulation, that will enable us to achieve better results.

## Methods

### Participants

Eight patients with intractable temporal lobe epilepsy participated in this study (four females, 15–51 years of age; mean and standard deviation of age  $27.8 \pm 11.6$  years) (Table 1). They were admitted to Osaka University Hospital from April 2015 to July 2019 and underwent intracranial electrode placement for an invasive EEG study. They had no swallowing disturbances, which was confirmed through a medical interview. All participants or their guardians were informed of the purpose and possible consequences of this study and written informed consent was obtained. The present study was approved by the Ethics Committee of Osaka University Hospital (Nos. 08061, 16469).

### Intracranial electrodes

For analysis, we chose planar-surface platinum grid electrodes ( $4 \times 5$  contacts array) that were placed over the lateral portion of the central sulcus corresponding to the orofacial cortex. The implanted electrodes that were

**Table 1.** Clinical profiles.

Participant	Sex	Age	Side	Number of orofacial contacts (total contacts)	Number of swallowing instances	Number of mouth opening instances	Number of water injections
P1	F	36	L	18 (68)	31	31	31
P2	F	30	L	20 (84)	41	41	41
P3	F	18	R	18 (55)	27	27	27
P4	M	24	L	15 (69)	34	34	34
P5	M	51	L	20 (72)	38	38	38
P6	M	28	R	20 (96)	27	27	27
P7	M	20	L	20 (94)	33	33	33
P8	F	15	L	20 (68)	37	37	37

M, Male; F, Female; R, Right; L, Left.

obtained from the CT images were overlaid onto the 3-dimensional brain renderings from the MRI volume that was created by FreeSurfer software (<https://surfer.nmr.mgh.harvard.edu>). We obtained the Montreal Neurological Institute (MNI) coordinates of the implanted contacts with Brainstorm software (<http://neuroimage.usc.edu/brainstorm/>). Details are provided in the Data S1.

### Task and swallowing monitoring

The participants were asked to sit on a chair and then open their mouths, and the examiner injected 2 mL of water into their mouths using a syringe.

For noninvasive swallowing detection, we used an electroglottograph (EGG), a microphone, and a motion-tracking system (Fig. 1A). A laryngograph (Laryngograph Ltd, London, UK) was used as an EGG and recorded the neck impedance changes associated with swallowing<sup>26</sup> (Fig. 1B). Sounds of swallowing due to the bolus passing through the pharynx were detected by a throat microphone<sup>27</sup> (Fig. 1C). We connected the throat microphone (Inkou mike; SH-12iK, NANZU, Shizuoka, Japan) to the laryngograph to record the swallowing sounds.

We captured the motion of the participants at 30 frames per second with the motion-tracking system, which was newly developed by us using Kinect v2 (Microsoft, Redmond, Washington, USA).<sup>11</sup>

An electric stimulator (NS-101; Unique Medical, Tokyo, Japan) supplied digital synchronizing signals to the laryngograph and a 128-channel digital EEG system. The multimodal data were synchronized and enabled us to noninvasively monitor the swallowing movements. Details are provided in the Data S1.

### Signal segmentation based on swallowing-related events

The swallowing onset time was determined at the time when the impedance waveform reached its peak (Fig. 1B). A previous study associated the neck impedance changes

with the following swallowing stages: stage I (the oral stage), stage II (the pharyngeal stage), and stage III (the esophageal stage). The time of the EGG peak corresponded to the beginning of the pharyngeal stage.<sup>27</sup> Since the oral phase is voluntarily controlled and the pharyngeal and esophageal phases are involuntarily controlled,<sup>1</sup> the swallowing onset time in this study corresponded to the transition time from voluntary swallowing to involuntary swallowing (Fig. 1B). We could also detect the time when the participant opened his/her mouth and when the examiner injected water into the participants' mouth using the video captured by the RGB camera of Kinect v2. Mouth triggers and water triggers, which corresponded to different times, were also inserted into iEEG data (the number of each trigger is shown in Table 1). Details are provided in the Data S1.

### Data acquisition and preprocessing

The iEEG signals were measured with a 128-channel digital EEG system (EEG 2000; Nihon Kohden Corporation, Tokyo, Japan). Before any further processing, contacts containing external noise or epileptic discharge were excluded. Throughout the following analyses, a band-pass filter using a two-way least-squares finite impulse response filter (pop\_eegfiltnew.m from the EEGLAB version 14.1.2b, <https://scn.ucsd.edu/eeGLAB/index.php>) was applied to the iEEG signals. Details are provided in the Data S1.

### Spectral analyses

A time-frequency analysis of the time-locked iEEG signals to each trigger was performed using EEGLAB with a frequency range from 1 to 330 Hz and spectral power (in dB) calculated in 0.5-Hz bins with 200 data points (from −5.0 to 2.5 sec in every 33-msec window). The baseline for the time-frequency analysis was initially 0.5 sec.

To create power contour maps, the power of each contact was constructed from the preprocessed iEEG signals using a band-pass filter in combination with the Hilbert



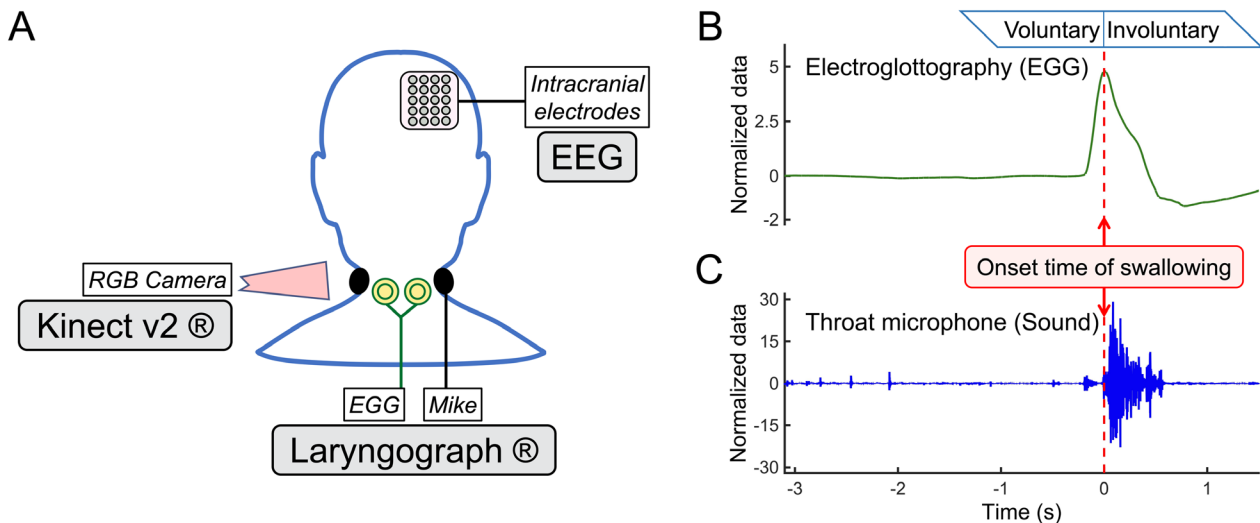


**Figure 1.** Multimodal data related to swallowing. (A) Intracranial electroencephalograms (EEGs) were recorded as participants swallowed. The swallowing was monitored by an RGB camera of Kinect v2, an electroglottograph (EGG), and a microphone of the laryngograph. Across-trials averaged impedance waveforms of an EGG (B) and a throat microphone (sound) (C) from one participant (P1) are shown. For analysis, the onset of swallowing was defined as the peak time of an impedance waveform. The onset time corresponds to the boundary time between voluntary and involuntary swallowing.

transformation.<sup>28</sup> We calculated the averaged power during a 0.5 sec time window, and the averaged power was normalized with the mean and standard deviation of the power during  $-5.0$  to  $-4.5$  sec of the swallowing triggers (Fig. 2 and Fig. S1B) or during  $-1.0$  to  $-0.5$  sec of the mouth triggers (Fig. 3).

### Extraction of contacts

Significant power increasing or decreasing contacts are indicated as filled white or black circles in Figure 3B. These contacts were plotted over the left hemisphere of the MNI normalized brain (Fig. 4A). The contacts attached to the right hemisphere were transposed to the left hemisphere.

The top 25% of contacts indicating a significant high  $\gamma$  power increase or a significant  $\beta$  power decrease were extracted and plotted on the left hemisphere of the MNI normalized brain (Fig. 5). These groups of contacts associated with each trigger were defined as mouth-related contacts (Mouth-C), water-related contacts (Water-C), and swallowing-related contacts (Swallow-C).

### Dynamic frequency power changes

We obtained averaged power waveforms of Mouth-C, Water-C, and Swallow-C relative to each trigger (mouth triggers, Mouth T; water triggers, Water T; swallowing triggers, Swallow T) in high  $\gamma$  (75–150 Hz) and  $\beta$  (13–30 Hz) bands. The power time series were normalized by

the power from base time ( $-1.0$  to  $-0.9$  sec of Mouth T). Details are provided in the Data S1.

### Correlation analysis

We calculated Pearson correlation coefficients between normalized  $\beta$  power at 0 sec of mouth triggers and sequential normalized  $\beta$  power from  $-1.5$  to 6 sec of mouth triggers. Correlation coefficients were calculated in each participant and then averaged. Using the Monte Carlo method, we set the threshold of correlation coefficients that achieved 80% statistical power.

### Statistics

For the statistical evaluation of neural oscillations, we used a permutation test.<sup>29</sup> For the comparison of the two groups, the Wilcoxon signed-rank test was used. For the correction of multiple comparisons, we used the Bonferroni correction or a family-wise error (FWE)-corrected threshold. For the comparison of three groups, we used a one-way analysis of variance (ANOVA). Details are provided in the Data S1.

### Data availability

All data that were generated or analyzed in this study are available from the corresponding authors upon reasonable request and after additional ethics approvals regarding data provision to individual institutions.

## Results

### Representative spatiotemporal oscillatory changes

The spatiotemporal oscillatory changes in a representative participant (Participant 1; P1) are shown in Figure 2. Averaged time-frequency maps around swallowing triggers from  $-4.5$  to  $2.0$  sec showed a high  $\gamma$  band ( $>50$  Hz) power increase within about  $-3.5$  to  $-2.0$  sec in the pre- and postcentral gyri (Fig. 2A and B). Simultaneously, the pre- and postcentral gyri also showed a decrease in the low-frequency band  $<50$  Hz. Within  $-2.0$  to  $0$  sec, a new

high  $\gamma$  power increase was observed in Channel (Ch) 9. After  $0$  sec, the pre- and postcentral gyri showed power increases in the low-frequency band  $<50$  Hz. Time-frequency maps showed that the lower frequency bands indicating obvious changes were  $\beta$  bands ( $13$ – $30$  Hz) (Fig. S1A).

A series of normalized power contour maps for the high  $\gamma$  band ( $75$ – $150$  Hz) and  $\beta$  band ( $13$ – $30$  Hz) were calculated from  $-4.5$  to  $2.5$  sec around swallowing triggers (Fig. 2C, Video S1). The location where the large high  $\gamma$  power increase appeared produced sequential changes. First, the large high  $\gamma$  power increase was observed in the pericentral gyri, especially for the

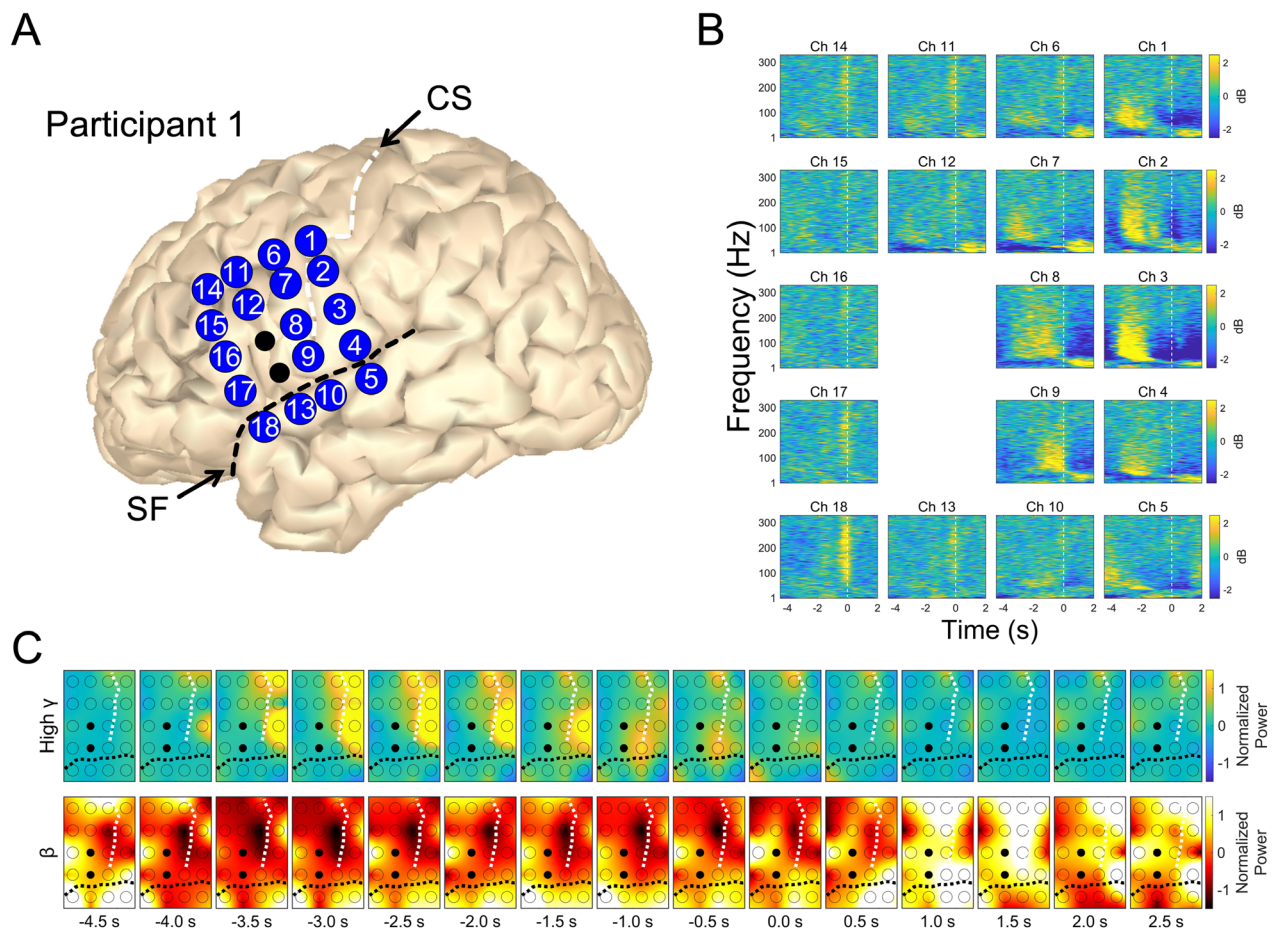


**Figure 2.** Temporal profiles of oscillatory changes associated with swallowing in Participant 1. (A) The reconstructed MR images. The numbers correspond to the contact numbers. (B) Averaged time-frequency maps are shown from  $-4.5$  to  $2.0$  sec around the swallowing trigger. These baselines of  $0.5$  sec duration range from  $-5.0$  to  $-4.5$  sec. High  $\gamma$  band power ( $>50$  Hz) increases specific to swallowing appeared in Channel (Ch) 9 attached to the subcentral area from  $-2.0$  to  $0$  sec. Within  $-3.5$  to  $-2.0$  sec, the time-frequency plots from the pre- and postcentral gyri showed high  $\gamma$  increases along with decreases in lower frequency band ( $< 50$  Hz) power (Ch 1, 2, 3, 4, 7, and 8). After  $0$  sec, the pre- and postcentral gyri showed the lower frequency power increase (Ch 1, 2, 3, 4, 6, 7, 8, 9, and 12). (C) Contour maps of normalized power in high  $\gamma$  ( $75$ – $150$  Hz) and  $\beta$  ( $13$ – $30$  Hz) bands are shown from  $-4.5$  to  $2.5$  sec every  $0.5$  sec interval around the swallowing trigger. The cortical areas in which the large power increased in the high  $\gamma$  band showed sequential changes. The contact that showed the largest high  $\gamma$  power increases immediately before swallowing onset time ( $-0.5$  sec) was Ch 9, attached to the subcentral area. The two black contacts were excluded because of severe noise contamination. The central sulcus (CS) and the Sylvian fissure (SF) are indicated by the white and black dotted lines, respectively.

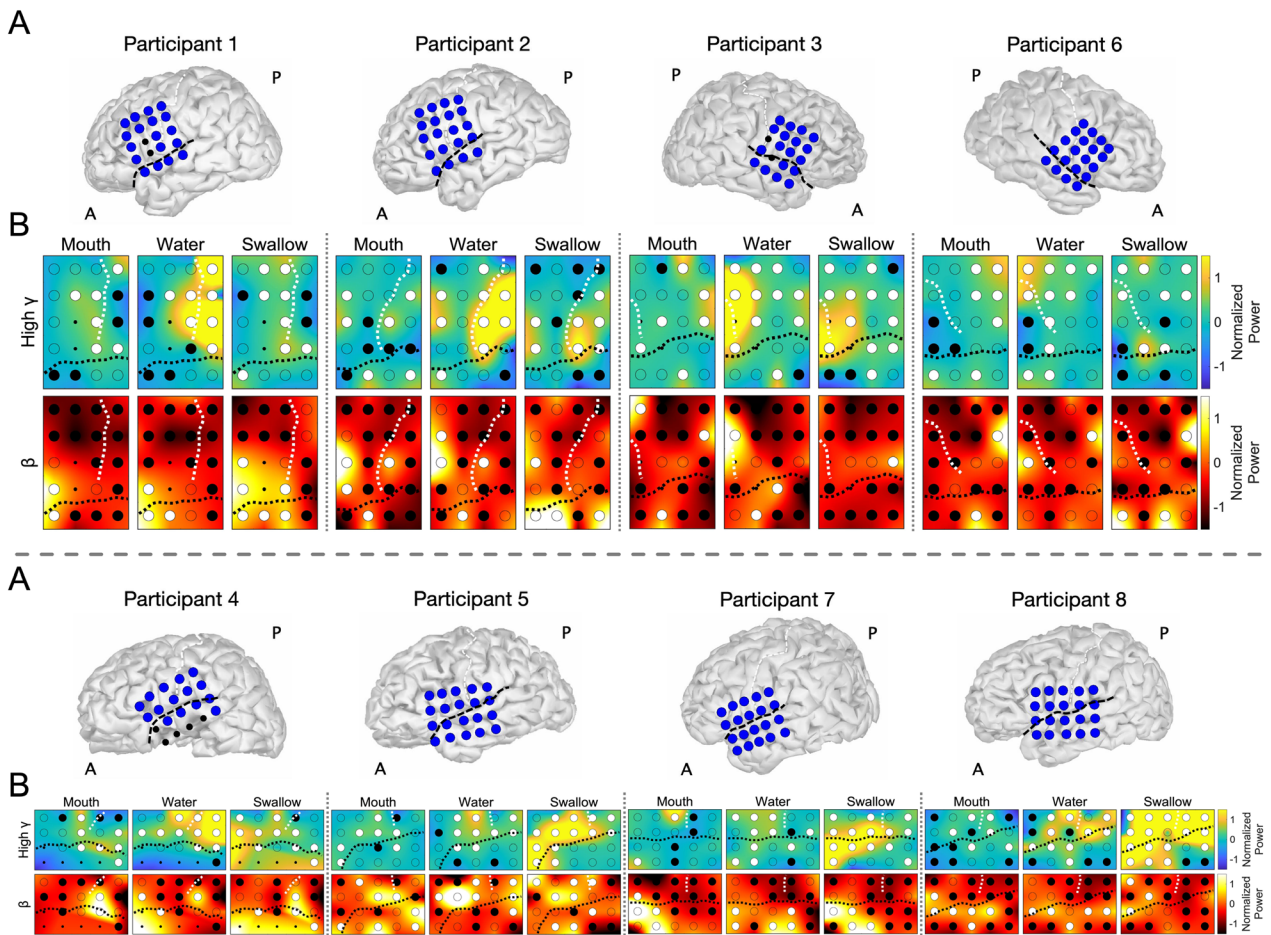


**Figure 3.** Power contour maps at the mouth, water, and swallowing triggers in high  $\gamma$  and  $\beta$  bands. (A) Reconstructed MR images for all participants. (B) The upper columns indicate high  $\gamma$  contour maps and the lower columns indicate  $\beta$  contour maps. Significant power increasing was indicated as white filled circles, and significant power decreasing was indicated as black-filled circles (corrected  $p < 0.05$ , single-sided permutation test with Bonferroni correction). Excluded contacts are indicated as small black-filled circles. The central sulcus and the Sylvian fissure are indicated by white and black dotted lines, respectively. Within the mouth, water, and swallowing, the main regions where high  $\gamma$  burst was observed were the precentral gyrus, the postcentral gyrus, and the cortex along the Sylvian fissure, respectively.  $\beta$  attenuation was observed in a wide area related to all three triggers.

postcentral gyrus during  $-4.0$  to  $-1.5$  sec. Subsequently, the subcentral area (the narrow gyrus between the caudolateral extreme of the central sulcus and the Sylvian fissure; Ch9) was the site where the large high  $\gamma$  power appeared within  $-1.0$  to  $-0.5$  sec. Conversely, before 0 sec, the  $\beta$  contour maps showed a power decrease in a wide area, especially for the precentral gyrus. After 0 sec, the previous high  $\gamma$  increase disappeared and the  $\beta$  power increase was observed over the same wide area.

Other lower frequency bands, including  $\delta$  (1–4 Hz),  $\theta$  (4–8 Hz), and  $\alpha$  (8–13 Hz) bands were also investigated; however, the spatial distribution patterns of lower frequency normalized power of these bands were obscure than that of the  $\beta$  band that showed different patterns between before and after swallowing (Fig. S1B). We

observed similar results among all participants; therefore, we focused on high  $\gamma$  and  $\beta$  bands for further analyses.

### High $\gamma$ and $\beta$ band contour maps with mouth, water, and swallowing triggers

For each participant, an averaged normalized power contour map of the high  $\gamma$  and  $\beta$  bands was created with mouth, water, and swallowing triggers (Fig. 3). We could observe a different spatial pattern of power increase (white filled circles; corrected  $p < 0.05$ , the single-sided permutation test with Bonferroni correction) in the high  $\gamma$  band within the three triggers. With the mouth trigger, a high  $\gamma$  burst was mainly observed in the precentral gyrus, and with the water trigger, the high  $\gamma$  burst was

observed in the pericentral gyri, especially in the postcentral gyrus. For the swallowing, high  $\gamma$  bursts appeared in the region along the Sylvian fissure.

Conversely, for the  $\beta$  band, it was difficult to identify a different spatial pattern. The power decrease (corrected  $p < 0.05$ , black-filled circles; the single-sided permutation test with Bonferroni correction) in the  $\beta$  band was widely observed for all three triggers.

## Profiles of high $\gamma$ and $\beta$ bands related to mouth, water, and swallowing triggers

### Power increasing versus power decreasing

All contacts showing power increase or decrease in Figure 3 were plotted on the left hemisphere of the MNI normalized brain (Fig. 4A). In the high  $\gamma$  band, the contacts of power increasing were plotted extensively in the water and swallowing groups rather than the mouth group. In the  $\beta$  band, the contacts of power decreasing were plotted extensively across all groups.

In the high  $\gamma$  band, the numbers of contacts indicating power increasing were significantly larger than those indicating power decreasing in water and swallowing groups (Fig. 4B) (corrected  $p = 0.012$  and  $0.023$ , the single-sided Wilcoxon signed-rank test with Bonferroni correction). In the  $\beta$  band, the numbers of contacts indicating power decreasing were significantly larger than those indicating power increasing in all three groups (corrected  $p = 0.023$ ,  $0.012$ , and  $0.035$ , the single-sided Wilcoxon signed-rank test with Bonferroni correction) (Fig. 4C).

We evaluated the differences across the three groups. The numbers of contacts indicating high  $\gamma$  burst were significantly different across the three groups ( $p = 0.001$ , one-way ANOVA) (Fig. 4D). However, the normalized power of high  $\gamma$  burst (Fig. 4E), the numbers of contacts indicating  $\beta$  attenuation (Fig. 4F), and the normalized power of  $\beta$  attenuation (Fig. 4G) showed no differences across groups (one-way ANOVA). These results indicated that high  $\gamma$  increasing and  $\beta$  decreasing were notably observed in all three groups, and different activities specific to mouth, water, and swallowing triggers appeared in high  $\gamma$  increasing rather than  $\beta$  decreasing.

### Spatial distribution

The top 25% of contacts indicating a significant increase in high  $\gamma$  power or degree of  $\beta$  attenuation were plotted over the MNI brain (Fig. 5). For the high  $\gamma$  power increasing, contacts related to water injection were active in the lateral portion of the central sulcus, and contacts related to swallowing were active in the regions along the Sylvian fissure. Contacts related to mouth opening were

found in the precentral gyrus and the ventrolateral prefrontal cortex (VLPFC) but were no better localized than the other groups.

In  $\beta$  power decreasing, contacts related to the mouth and water groups were mainly localized in the VLPFC, and the localization appeared to be less specific in the swallowing group. This result indicated that high  $\gamma$  activities were better localized rather than  $\beta$  activities, and the high  $\gamma$  localization might reflect differences in neural processing.

### Dynamic power changes

For high  $\gamma$  and  $\beta$  bands, we used three groups (Mouth-C, Water-C, and Swallow-C) and three trigger groups to derive nine different power plots (Fig. 6). Data obtained from Mouth T, Water T, and Swallow T were arranged in chronological order.

Around 0 sec of Mouth T, only Mouth-C showed a high  $\gamma$  burst. Around 0 sec of Water T, Water-C showed a notable high  $\gamma$  burst. At 0 sec of Swallow T, in Swallow-C, the high  $\gamma$  burst reached the peak value. In high  $\gamma$  activities, at 0 sec of all triggers, there were significant differences across Mouth-C, Water-C, and Swallow-C (corrected  $p = 0.040$  in Mouth T, corrected  $p < 0.001$  in Water T, and corrected  $p = 0.001$  in Swallow T, one-way ANOVA with Bonferroni correction). The high  $\gamma$  burst showed statistical significance because they were bigger than the FWE-corrected threshold (Fig. 6A).

Moreover, the 0 sec of the Swallow T corresponded to the boundary between voluntary swallowing and involuntary swallowing (red wedge arrow in Fig. 6A). Therefore, our results showed that during the voluntary phase, high  $\gamma$  activities were increasing until completion of the voluntary swallowing, and subsequently, the high  $\gamma$  activities decreased. Furthermore, we plotted the dynamic change of swallowing-related high  $\gamma$  normalized power calculated from both the left and right hemispheres. A similar pattern was observed in both hemispheres (Fig. S2A). The normalized power of high  $\gamma$  band related to swallowing was larger in the right hemisphere than that in the left hemisphere (Fig. S2B).

Conversely,  $\beta$  power showed similar patterns for each trigger (Fig. 6B). Except for Mouth T (corrected  $p = 0.004$ , one-way ANOVA with Bonferroni correction), there were no significant changes at 0 sec of Water T and Swallow T across contact groups (one-way ANOVA with Bonferroni correction). In Mouth T,  $\beta$  power was suppressed before 0 sec. For Water T,  $\beta$  power remained inhibited, and with Swallowing T,  $\beta$  attenuation continued up to about 0.5 sec, thereafter  $\beta$  power rebounded. The  $\beta$  attenuation showed statistical significance because they were lesser than the FWE-corrected threshold.



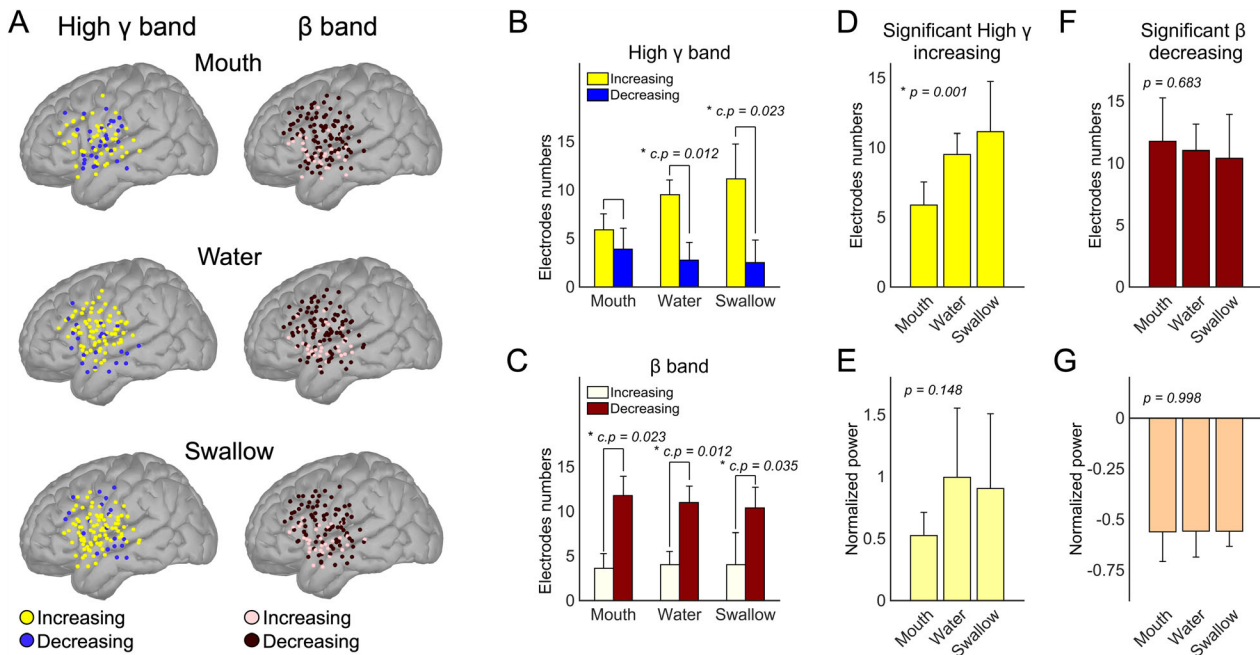


**Figure 4.** Profiles of high  $\gamma$  and  $\beta$  bands related to mouth, water, and swallowing triggers. (A) For each trigger group, contacts indicating significant power increases or decreases in high  $\gamma$  or  $\beta$  band were plotted over the left hemisphere of the MNI brain. In the high  $\gamma$  band, a power increase was notable, and in the  $\beta$  band, power decreasing was notable and extensive. (B) Within the mouth, water, and swallowing groups, the numbers of contacts were compared between the two groups including power increasing or power decreasing (single-sided Wilcoxon signed-rank test).  $p$  values were corrected with Bonferroni correction and significant  $p$  values ( $< 0.05$ ) are indicated by an asterisk (corrected  $p$ : c.p). In the high  $\gamma$  band, the number of increasing contacts was significantly larger than that of decreasing contacts in the water and swallowing groups. (C) In the  $\beta$  band, the numbers of decreasing contacts were significantly larger in all groups. In high  $\gamma$  power increasing contacts or  $\beta$  power decreasing contacts, the numbers of contacts and the degree of normalized power changing were compared across the mouth, water, and swallowing groups (significant  $p$  values ( $< 0.05$ ) are indicated with an asterisk, one-way ANOVA) (high  $\gamma$  band in D and E,  $\beta$  band in F and G; the numbers of contacts in D and F, the degree of power changing in E and G). In the numbers of contacts with high  $\gamma$  increases, there were significant differences. There were no statistical differences in the normalized power changes in high  $\gamma$  band (E) and  $\beta$  band (G), and in the numbers of contacts in  $\beta$  band (F). The error bars indicate standard deviation (B–G).

## Time to change

We compared the lead time when  $\beta$  or high  $\gamma$  power began to change between each trigger with each related contact. For the mouth trigger,  $\beta$  decreasing preceded the high  $\gamma$  increasing, but changes were not significant (the single-sided Wilcoxon signed-rank test) (Fig. 7A). The lead time of the high  $\gamma$  increasing showed significant differences across mouth, water, and swallowing groups ( $p = 0.004$ , one-way ANOVA) (Fig. 7B). The time of the swallow was the earliest between the three groups. Even in the water, the beginning time of high  $\gamma$  burst preceded the 0 sec of water triggers.

## $\beta$ attenuation

To investigate  $\beta$  activities, we plotted the normalized  $\beta$  power from  $-1.5$  to  $6$  sec of mouth triggers (Fig. 8A). The  $\beta$  attenuation at 0 sec of mouth triggers was maintained up to about 4 sec, after which the  $\beta$  power

rebounded. We investigated the correlation between  $\beta$  normalized power at 0 sec of the mouth triggers (gray mesh area in Fig. 8)—sequential  $\beta$  normalized power. The sequential correlation coefficients ( $r$ ) were shown (Fig. 8B). Significant positive correlation above the threshold (red dashed line in Fig. 8B) that meant 80% statistical power was observed until rebound  $\beta$  appearance. The results indicated that the  $\beta$  attenuation was induced by mouth opening, and the continuous  $\beta$  attenuation was correlated to the mouth-related  $\beta$  attenuation.

## Discussion

The swallowing-oral phase is voluntarily controlled, whereas the swallowing-pharyngeal and esophageal phases are involuntarily controlled.<sup>1</sup> We inserted the swallowing trigger at the boundary time between the oral and the pharyngeal phases.<sup>27</sup> Therefore, our swallowing triggers were inserted between the transition from voluntary to involuntary swallowing. In the present study, during the

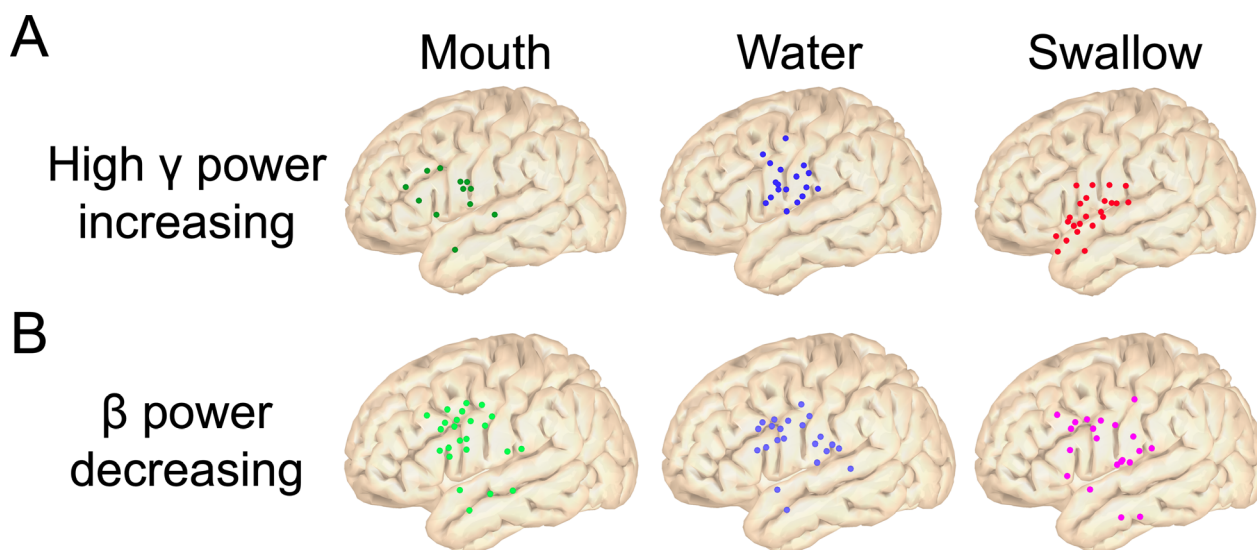


**Figure 5.** Spatial profile related to mouth, water, and swallowing trigger groups. The top 25% contacts indicating significant high  $\gamma$  power increases or  $\beta$  decreases were plotted over the left hemisphere of the MNI brain. In high  $\gamma$  increases, mouth-related contacts were observed in the precentral gyrus and the ventrolateral prefrontal cortex (VLPFC). Water-related contacts were observed in the lateral portion of the central sulcus, and swallowing-related contacts were observed on the regions along the Sylvian fissure. In  $\beta$  decreasing, mouth- and water-related contacts were mainly localized in the VLPFC, and the localization loosened in the swallowing group.

voluntary swallowing phase, the high  $\gamma$  bursts appeared; however, in conjunction with the completion of voluntary swallowing, the high  $\gamma$  activity decreased. A previous ECoG study reported that the cerebral cortex is involved in voluntary swallowing to a greater degree than in swallowing execution.<sup>30</sup> Our finding that the high  $\gamma$  burst related to swallowing achieved a peak at the transition between voluntary and involuntary swallowing might indicate a neural mechanism: the main drive for swallowing switched from the cerebral cortex to the brainstem. Moreover, damage to cortical areas, such as the Brodmann's areas (BA) 43 and 44, is clinically known to cause dysphagia,<sup>31,32</sup> and the opercular syndrome (Foix–Chavany–Marie syndrome) reveals that the voluntary phase of swallowing is severely affected, while reflex swallowing is preserved.<sup>32</sup> Taken together, these findings imply that the cortex plays a crucial role in execution of voluntary swallowing rather than involuntary swallowing.

Previous studies have reported a hemispheric dominance for swallowing.<sup>17,20,33–35</sup> Teismann et al. demonstrated that there was a shift in hemispheric dominance during volitional swallowing in which the early (oral) stage of swallowing is driven by the left hemisphere and cortical activation shifts to bilateral then eventually to the right hemisphere at later (pharyngeal and esophageal) stages of swallowing.<sup>33</sup> However, in this study, high  $\gamma$  normalized power achieved higher values in the right hemisphere rather than the left hemisphere. We thought that this different result might be due to our low sample

size (two right sides and six left sides) and therefore, we cannot comment on the hemispheric dominance for swallowing. [Correction added on May 25, 2021 after first online publication: The preceding sentence was revised from "... (two right sides and two left sides)..."].

We could demonstrate that using high  $\gamma$  activities, different cortical areas associated with swallowing were activated. Mouth opening-associated high  $\gamma$  burst appeared mainly in the lateral precentral gyrus and in the VLPFC, and these regions have been reported to be actively involved in orofacial motor action.<sup>36,37</sup> Water-related high  $\gamma$  bursts were observed in the lateral portion along the central sulcus, which are known to be activated by tactile stimulation of the buccal mucosa.<sup>38</sup> Swallowing-related high  $\gamma$  bursts were observed in regions along the Sylvian fissure, including the subcentral area (BA 43) and the frontal operculum (BA 44). Previous studies have reported that swallowing activates the subcentral area<sup>18,30,39</sup> and the frontal operculum.<sup>17,20,40</sup> The cortical areas along the Sylvian fissure, including BA 43 and BA 44, may have the potential for novel targets of neuromodulation that aim at recovery from dysphagia.

The subcentral area was also activated by a communication function, such as vocal productions in response to acoustic perturbations<sup>41</sup> and eye-to-eye contact.<sup>42</sup> The frontal operculum (BA 44) is generally known as a key component of language production.<sup>37</sup> Monkeys possess an area comparable to human BA 44, and it has been hypothesized that BA 44 might have evolved as

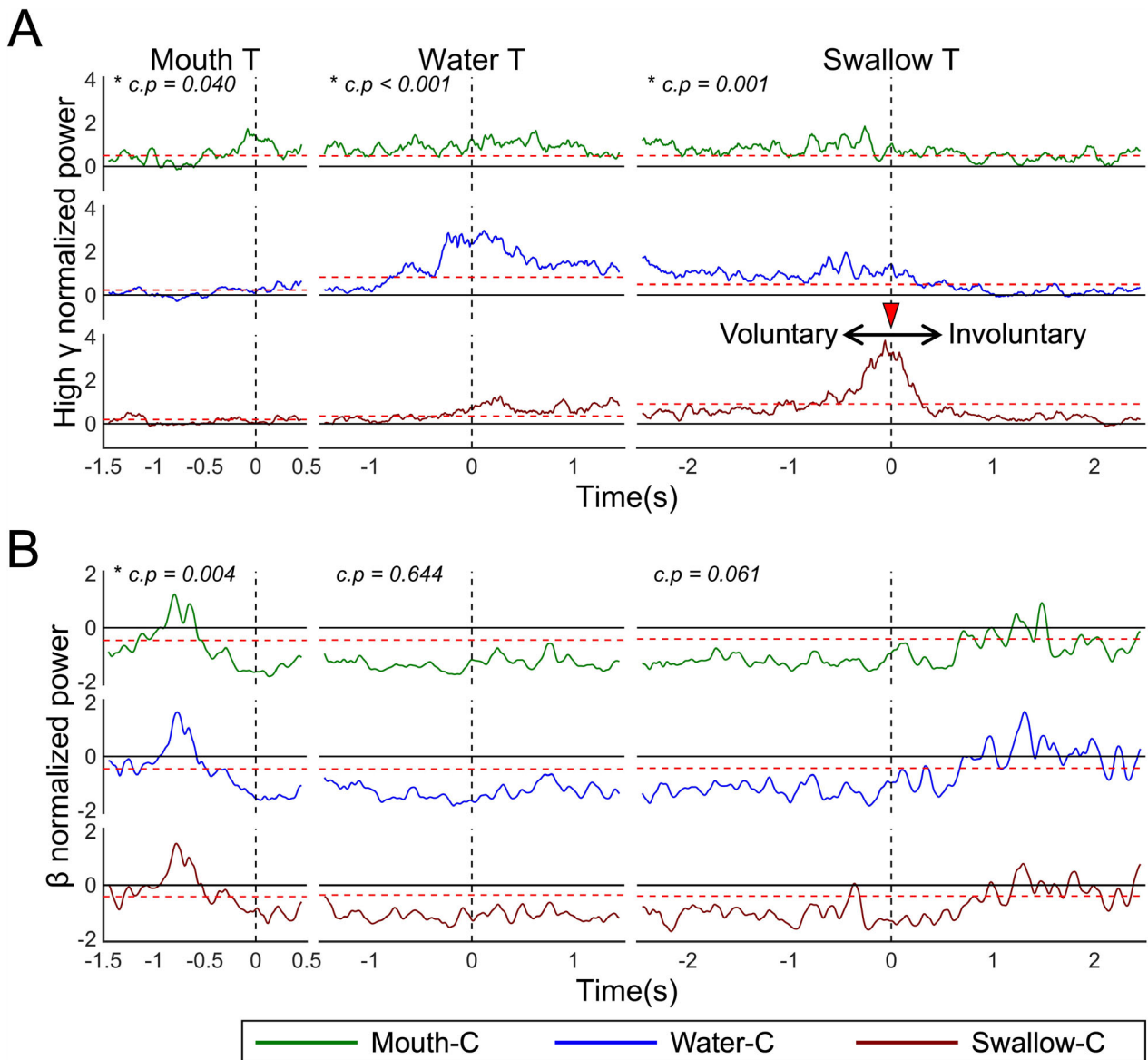


**Figure 6.** Temporal profile related to swallowing, mouth, and water trigger groups. Averaged normalized power of high  $\gamma$  band (A) and  $\beta$  band (B) calculated from top 25% contacts, which showed significant power changes (Fig. 5). The contact groups were indicated as Mouth-C, Water-C, and Swallow-C, colored by green, blue, and red, respectively. At 0 sec of mouth triggers (Mouth T), only Mouth-C showed a high  $\gamma$  burst not Water-C and Swallow-C. At 0 sec of Water T, Water-C showed notably high  $\gamma$  bursts. With Swallow T, Swallow-C showed high  $\gamma$  power increasing and achieved a peak at 0 sec (red wedge arrow). After that, the power decreased. The 0 sec of Swallow T corresponded to the transition time from voluntary swallowing to involuntary swallowing. In the  $\beta$  band, three contact groups showed the same pattern as the  $\beta$  power decreases from Mouth T, and the attenuation was maintained until about 1.0 sec of Swallow T. Red dotted lines are FWE-corrected threshold. We evaluated the normalized power at 0 sec of each trigger across Mouth-C, Water-C, and Swallow-C using one-way ANOVA. There were significant differences in all triggers with high  $\gamma$  band and in Mouth T with  $\beta$  band.

an area exercising high-level controls over orofacial activities including those related to communicative acts, and that, in the human brain, the BA 44 evolved to control the motor aspects of speech.<sup>43</sup> Therefore, it is feasible that both BA 43 and 44 are involved in communication.

In the process of evolution, the early jawless vertebrates were able to swallow,<sup>44</sup> and next, jawed vertebrates came to be able to masticate before swallowing. The orofacial muscular movements associated with mastication were eventually diverted to other functions, such as facial expressions for communication. Finally, in humans,

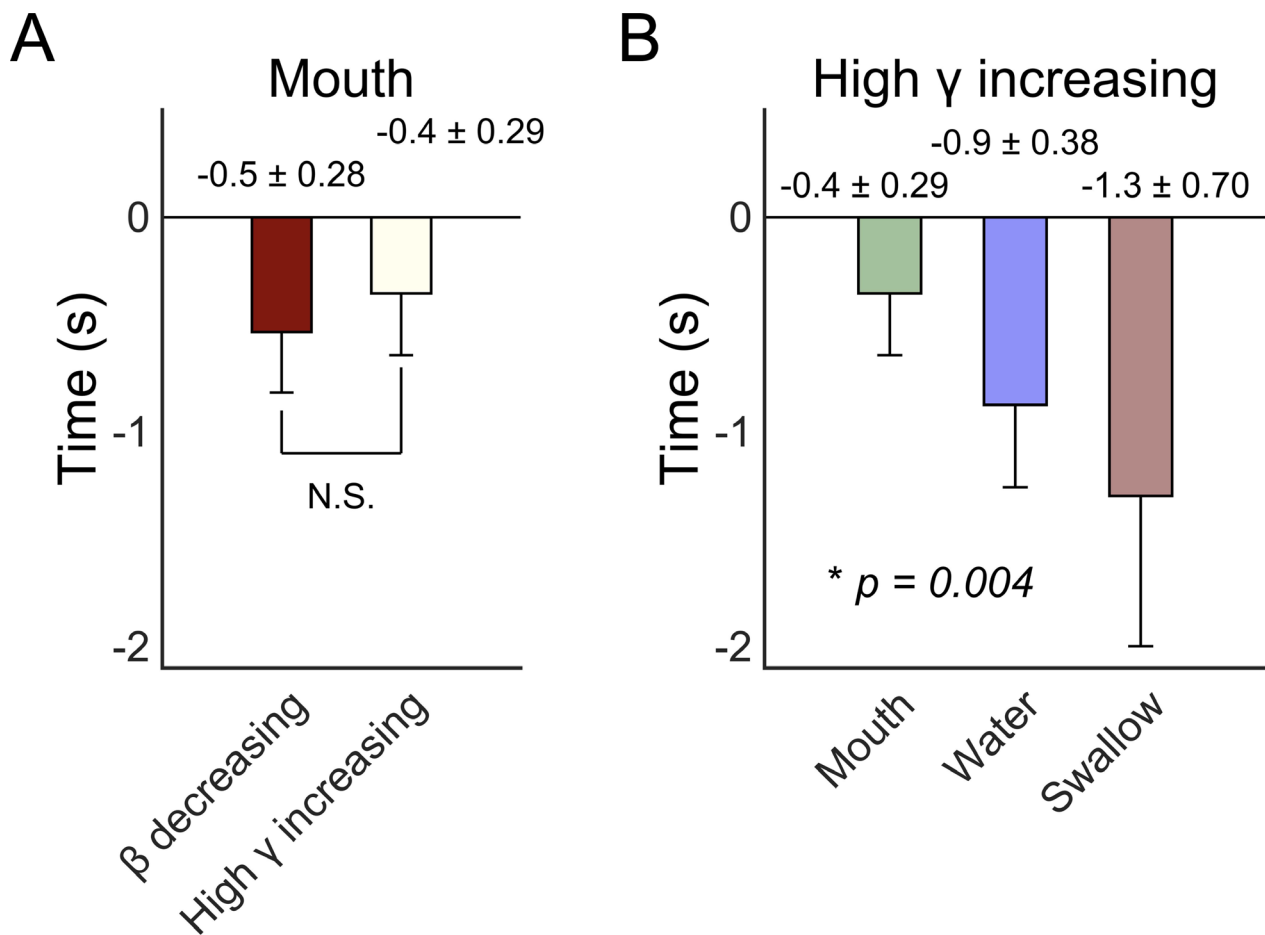


**Figure 7.** The beginning time of power changes. The beginning time of power changes for each band with each trigger was compared. In mouth triggers, there were no statistically significant differences between  $\beta$  decreasing and high  $\gamma$  increasing (single-sided Wilcoxon signed-rank test) (A). The time when swallowing-related high  $\gamma$  started to increase was the earliest, and statistically significant differences were observed across the mouth, water, and swallowing triggers (one-way ANOVA) (B). The error bars indicate standard deviation.

orofacial muscular movements were used for motor language. Therefore, we think that the cortex associated with swallowing is quite extensive given the early acquisition in the evolutionary process, and now overlaps areas that relate to mastication, facial expression, and speech which were originally involved in orofacial muscular movement.

The area of  $\beta$  attenuation was extensive, and  $\beta$  attenuation was similar for the mouth, water, and swallowing events. In a previous study,  $\beta$  event-related desynchronizations (ERDs) in the lateral pericentral gyri were induced by tongue movement and swallowing.<sup>20</sup> In our study,  $\beta$  attenuation was invoked associated with mouth opening, and the  $\beta$  band attenuation remained until the completion of the swallowing movement. Furthermore, continuous  $\beta$  band attenuation positively correlated with the mouth movement-associated  $\beta$  attenuation; therefore, we inferred that  $\beta$  attenuation observed in both water and swallowing events was induced by mouth

movements. Mouth movement induced  $\beta$  attenuation simultaneously with high  $\gamma$  burst, which was consistent with the ECoG findings demonstrating that motor behavior induces high  $\gamma$  activities along with decreases in  $\beta$  power.<sup>23,36,45,46</sup> Moreover, this  $\beta$  attenuation was released after the completion of the swallowing, and  $\beta$  power increased. This re-activation is known as rebounded  $\beta$ .<sup>47</sup> The  $\beta$  attenuation and subsequent rebound observed in this study agree with previous findings.

The MEG study by Dziewas et al. showed that both reflexive and volitional swallowing induced  $\beta$  ERD in the mid-lateral primary sensorimotor cortex, and  $\beta$  ERD occurred in more medial parts of the primary sensorimotor cortex during reflexive swallowing rather than during volitional swallowing.<sup>20</sup> In this study, the  $\beta$  attenuation was also observed in the lateral region of the central sulcus during swallowing; however, we inferred that the  $\beta$  attenuation was related to mouth movement. We



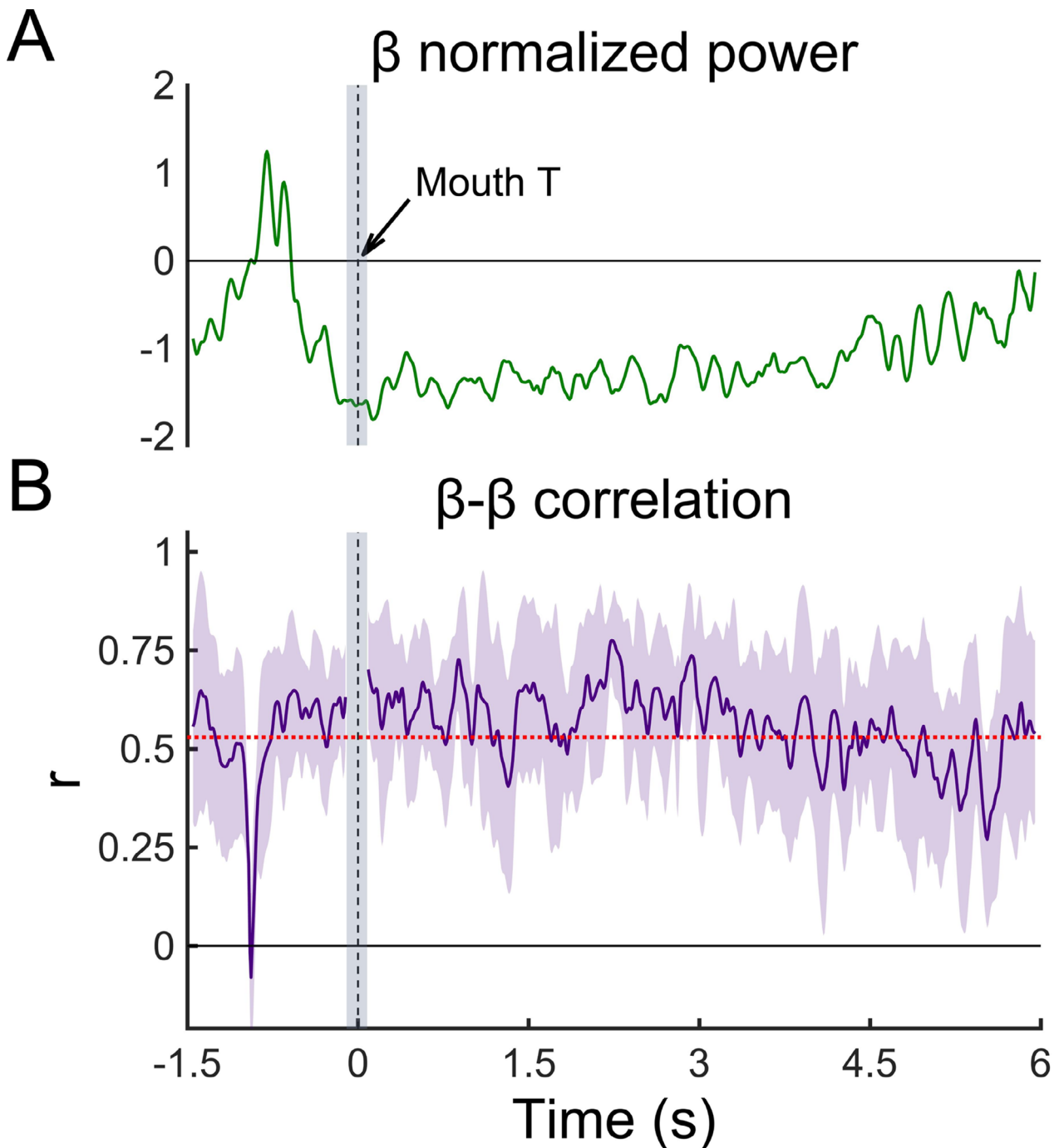


**Figure 8.** Mouth-related  $\beta$  band activities. Normalized power changes of  $\beta$  band with mouth triggers from  $-1.5$  to  $6.0$  sec were presented (A).  $\beta$  normalized power was suppressed before  $0$  sec, and remained inhibited, and, thereafter rebounded. Correlation coefficients ( $r$ ) between  $\beta$  normalized power at  $0$  sec (gray mesh area) and  $\beta$  normalized power at a certain time during the period from  $-1.5$  to  $6$  sec were shown (B). The dotted red line is the threshold that showed 80% statistical power. During  $\beta$  attenuation, positive correlations that were above the threshold were observed. During  $\beta$  rebound, the positive correlations became weak. The error bars indicate 95% confidence intervals.

figured that the differences were due to the brain regions to be investigated. MEG studies enabled us to investigate the whole brain; however, studies using ECoG, such as

our study, focus only on a narrow area where intracranial electrodes are placed. Therefore, we cannot comment on the  $\beta$  activities in the mid-lateral primary

sensorimotor cortex where intracranial electrodes were not placed.

Somatosensory stimulation evokes high  $\gamma$  activities in the sensory-motor cortex,<sup>48</sup> and we expected that water-associated high  $\gamma$  bursts would appear after the water triggers; however, contrary to our expectation, the beginning of the water-related high  $\gamma$  burst was 0.9 sec earlier than the onset time of the water trigger. The onset time of the water trigger corresponded to the time when the water bolus was injected by a syringe, which was fixed onto the lip. We inferred that the time lag was a result of the somatosensory input from the lip on which a syringe was placed. The high  $\gamma$  burst of the Water-C was observed notably only with Water T, and not at Mouth T and Swallow T. We concluded that the notably high  $\gamma$  bursts were evoked by somatosensory input from lip or mouth mucosa.

Our study has several limitations. First, we focused only on the orofacial cortex, which is where the lateral region of the central sulcus is located. Multiple cortices are activated during swallowing<sup>2</sup>; however, our study could not demonstrate cortical activities other than in the orofacial region. Second, in this study, we divided swallowing events into three parts (mouth opening, water injection, and swallowing), and discussed motor and somatosensory neural processing. For more precise analysis, we may need to treat these as separate events, that is, mouth movement only, water injection into the mouth only, and swallowing only. Third, we inferred the switching mechanism of the swallowing-related main driving force from the cortex to the brain stem. In the future, simultaneous recording of the cortex and the brain stem may be needed to reveal how the swallowing-related interaction between them works.

## Conclusion

With high  $\gamma$  activities, we distinguished the discrete cortical activities that are involved in swallowing and demonstrated that the cortical areas that are specific to swallowing are the regions along the Sylvian fissure including the subcentral area and the frontal operculum. Swallowing-related high  $\gamma$  activities that achieved the peak at the boundary time between voluntary and involuntary swallowing may represent the neural processing of switching from the cortex to the brainstem involved in swallowing execution.

## Acknowledgment

This work was supported by the Japan Society for the Promotion of Science (JSPS) KAKENHI [Grant nos. JP26282165 (Masayuki Hirata), JP18H04166 (Masayuki Hirata), JP18K18366 (Hiroaki Hashimoto)], by the

Ministry of Internal Affairs and Communications (Masayuki Hirata), by a grant from the National Institute of Information and Communications Technology (NICT) (Masayuki Hirata), and by a grant from the National Institute of Dental and Craniofacial Research (NIDCR)-RO1 DE023816 (Kazutaka Takahashi).

## Conflict of Interest

No author has any conflict of interest to disclose.

## Author Contributions

M.H. designed the study. H.H. performed the experiments, assisted with the epileptic medical treatment, created the MATLAB program and analyzed the data, created all the figures and tables, and was primarily responsible for writing the manuscript. F.Y., H.M., and M.H. assisted in the acquisition of the measurements. S.K. developed some devices to help with the measurements. H.K., S.O., N.T., H.M.K., and M.H. performed the epilepsy surgery, and Ta. Ya. assisted with the epileptic medical treatment. M.H., K.T., and Ta. Ya advised H.H. on scientific matters. M.H. and K.T. revised the manuscript. To. Yo., H.K., and M.H. supervised the experiments and analyses. All authors reviewed the manuscript.

## References

1. Jean A. Brain stem control of swallowing: neuronal network and cellular mechanisms. *Physiol Rev* 2001;81:929–969.
2. Ertekin C, Aydogdu I. Neurophysiology of swallowing. *Clin Neurophysiol* 2003;114:2226–2244.
3. Smithard DG, Smeeton NC, Wolfe CD. Long-term outcome after stroke: does dysphagia matter? *Age Ageing* 2007;36:90–94.
4. Boccardi V, Ruggiero C, Patrìti A, Marano L. Diagnostic assessment and management of dysphagia in patients with Alzheimer's disease. *J Alzheimers Dis* 2016;50:947–955.
5. Speyer R, Baijens L, Heijnen M, Zwijnenberg I. Effects of therapy in oropharyngeal dysphagia by speech and language therapists: a systematic review. *Dysphagia* 2010;25:40–65.
6. Suntrup S, Teismann I, Wollbrink A, et al. Pharyngeal electrical stimulation can modulate swallowing in cortical processing and behavior - magnetoencephalographic evidence. *NeuroImage* 2015;104:117–124.
7. Ludlow CL, Humbert I, Saxon K, et al. Effects of surface electrical stimulation both at rest and during swallowing in chronic pharyngeal Dysphagia. *Dysphagia* 2007;22:1–10.
8. Verin E, Leroi AM. Poststroke dysphagia rehabilitation by repetitive transcranial magnetic stimulation: a noncontrolled pilot study. *Dysphagia* 2009;24:204–210.

9. Vasant DH, Mistry S, Michou E, et al. Transcranial direct current stimulation reverses neurophysiological and behavioural effects of focal inhibition of human pharyngeal motor cortex on swallowing. *J Physiol* 2014;592:695–709.
10. Sasegbon A, Cheng I, Zhang M, Hamdy S. Advances in the use of neuromodulation for neurogenic dysphagia: mechanisms and therapeutic application of pharyngeal electrical stimulation, transcranial magnetic stimulation, and transcranial direct current stimulation. *Am J Speech Lang Pathol* 2020;29(2S):1044–1064.
11. Hashimoto H, Hirata M, Takahashi K, et al. Non-invasive quantification of human swallowing using a simple motion tracking system. *Sci Rep* 2018;8:5095.
12. Hashimoto H, Kameda S, Maezawa H, et al. A swallowing decoder based on deep transfer learning: AlexNet classification of the intracranial electrocorticogram. *Int J Neural Syst* 2020;2050056. <https://doi.org/10.1142/S0129065720500562>
13. Yang H, Guan C, Chua KS, et al. Detection of motor imagery of swallow EEG signals based on the dual-tree complex wavelet transform and adaptive model selection. *J Neural Eng* 2014;11:035016.
14. Hamdy S, Rothwell JC, Brooks DJ, et al. Identification of the cerebral loci processing human swallowing with H2 (15)O PET activation. *J Neurophysiol* 1999;81:1917–1926.
15. Kober SE, Wood G. Changes in hemodynamic signals accompanying motor imagery and motor execution of swallowing: a near-infrared spectroscopy study. *NeuroImage* 2014;93(Pt 1):1–10.
16. Hamdy S, Aziz Q, Rothwell JC, et al. The cortical topography of human swallowing musculature in health and disease. *Nat Med* 1996;2:1217–1224.
17. Hamdy S, Mikulis DJ, Crawley A, et al. Cortical activation during human volitional swallowing: an event-related fMRI study. *Am J Physiol* 1999;277(1 Pt 1):G219–G225.
18. Toogood JA, Smith RC, Stevens TK, et al. Swallowing preparation and execution: insights from a delayed-response functional magnetic resonance imaging (fMRI) study. *Dysphagia* 2017;32:526–541.
19. Furlong PL, Hobson AR, Aziz Q, et al. Dissociating the spatio-temporal characteristics of cortical neuronal activity associated with human volitional swallowing in the healthy adult brain. *NeuroImage* 2004;22:1447–1455.
20. Dziewas R, Soros P, Ishii R, et al. Neuroimaging evidence for cortical involvement in the preparation and in the act of swallowing. *NeuroImage* 2003;20:135–144.
21. Aine CJ. A conceptual overview and critique of functional neuroimaging techniques in humans: I. MRI/fMRI and PET. *Crit Rev Neurobiol* 1995;9:229–309.
22. Nascimento WV, Cassiani RA, Santos CM, Dantas RO. Effect of bolus volume and consistency on swallowing events duration in healthy subjects. *J Neurogastroenterol Motil* 2015;21:78.
23. Crone NE, Miglioretti DL, Gordon B, Lesser RP. Functional mapping of human sensorimotor cortex with electrocorticographic spectral analysis. II. Event-related synchronization in the gamma band. *Brain* 1998;121(Pt 12):2301–2315.
24. Canolty RT, Edwards E, Dalal SS, et al. High gamma power is phase-locked to theta oscillations in human neocortex. *Science* 2006;313:1626–1628.
25. Hashimoto H, Hasegawa Y, Araki T, et al. Non-invasive detection of language-related prefrontal high gamma band activity with beamforming MEG. *Sci Rep* 2017;7:14262.
26. Firmin H, Reilly S, Fourcin A. Non-invasive monitoring of reflexive swallowing. *Speech Hear Lang* 1997;10:171–184.
27. Kusahara T, Nakamura T, Shirakawa Y, et al. Impedance pharyngography to assess swallowing function. *J Int Med Res* 2004;32:608–616.
28. Cohen MX. Assessing transient cross-frequency coupling in EEG data. *J Neurosci Methods* 2008;168:494–499.
29. Maris E, Oostenveld R. Nonparametric statistical testing of EEG- and MEG-data. *J Neurosci Methods* 2007;164:177–190.
30. Satow T, Ikeda A, Yamamoto J, et al. Role of primary sensorimotor cortex and supplementary motor area in volitional swallowing: a movement-related cortical potential study. *Am J Physiol Gastrointest Liver Physiol* 2004;287:G459–G470.
31. Alberts MJ, Horner J, Gray L, Brazer SR. Aspiration after stroke: lesion analysis by brain MRI. *Dysphagia* 1992;7:170–173.
32. Baijens LW, Speyer R, Roodenburg N, Manni JJ. The effects of neuromuscular electrical stimulation for dysphagia in opercular syndrome: a case study. *Eur Arch Otorhinolaryngol* 2008;265:825–830.
33. Teismann IK, Dziewas R, Steinstraeter O, Pantev C. Time-dependent hemispheric shift of the cortical control of volitional swallowing. *Hum Brain Mapp* 2009;30:92–100.
34. Mosier KM, Liu W-C, Maldjian JA, et al. Lateralization of cortical function in swallowing: a functional MR imaging study. *Am J Neuroradiol* 1999;20:1520–1526.
35. Soros P, Inamoto Y, Martin RE. Functional brain imaging of swallowing: an activation likelihood estimation meta-analysis. *Hum Brain Mapp* 2009;30:2426–2439.
36. Miller KJ, Leuthardt EC, Schalk G, et al. Spectral changes in cortical surface potentials during motor movement. *J Neurosci* 2007;27:2424–2432.
37. Loh KK, Procyk E, Neveu R, et al. Cognitive control of orofacial motor and vocal responses in the ventrolateral and dorsomedial human frontal cortex. *P Natl Acad Sci USA* 2020;117:4994–5005.
38. Miyaji H, Hironaga N, Umezaki T, et al. Neuromagnetic detection of the laryngeal area: sensory-evoked fields to air-puff stimulation. *NeuroImage* 2014;88:162–169.
39. Martin RE, MacIntosh BJ, Smith RC, et al. Cerebral areas processing swallowing and tongue movement are

- overlapping but distinct: a functional magnetic resonance imaging study. *J Neurophysiol* 2004;92:2428–2443.
40. Lowell SY, Poletto CJ, Knorr-Chung BR, et al. Sensory stimulation activates both motor and sensory components of the swallowing system. *NeuroImage* 2008;42:285–295.
  41. Chang EF, Niziolek CA, Knight RT, et al. Human cortical sensorimotor network underlying feedback control of vocal pitch. *Proc Natl Acad Sci USA* 2013;110:2653–2658.
  42. Hirsch J, Zhang X, Noah JA, Ono Y. Frontal temporal and parietal systems synchronize within and across brains during live eye-to-eye contact. *NeuroImage* 2017;157:314–330.
  43. Petrides M, Cadoret G, Mackey S. Orofacial somatomotor responses in the macaque monkey homologue of Broca's area. *Nature* 2005;435:1235–1238.
  44. Clark AJ, Uyeno TA. Feeding in jawless fishes. Feeding in vertebrates. Cham, Switzerland: Springer; 2019:189–230.
  45. Dalal SS, Guggisberg AG, Edwards E, et al. Five-dimensional neuroimaging: localization of the time-frequency dynamics of cortical activity. *NeuroImage* 2008;40:1686–1700.
  46. Yanagisawa T, Hirata M, Saitoh Y, et al. Electrocorticographic control of a prosthetic arm in paralyzed patients. *Ann Neurol* 2012;71:353–361.
  47. Salmelin R, Hamalainen M, Kajola M, Hari R. Functional segregation of movement-related rhythmic activity in the human brain. *NeuroImage* 1995;2:237–243.
  48. Hirata M, Kato A, Taniguchi M, et al. Frequency-dependent spatial distribution of human somatosensory evoked neuromagnetic fields. *Neurosci Lett* 2002;318:73–76.

## Supporting Information

Additional supporting information may be found online in the Supporting Information section at the end of the article.

**Figure S1.** Lower frequency activities acquired from Participant 1 (P1).

**Figure S2.** High  $\gamma$  changes calculated from the left and the right hemispheres.

**Data S1.** Supplementary methods.

**Video S1.** Temporal profile of high  $\gamma$  and  $\beta$  band power related to swallowing.